

1 **Simultaneous sludge minimization, biological phosphorous removal and membrane fouling**  
2 **mitigation in a novel plant layout for MBR**

3  
4 Santo Fabio Corsino<sup>a\*</sup>, Taissa Silva de Oliveira<sup>a</sup>, Daniele Di Trapani<sup>a</sup>, Michele Torregrossa<sup>a</sup>,  
5 Gaspare Viviani<sup>a</sup>

6  
7 <sup>a</sup>Dipartimento di Ingegneria,  
8 Università di Palermo, Viale delle Scienze, 90128 Palermo, Italy

9  
10  
11 \*Corresponding author: tel: +39 09123896555; fax: +39 09123860810

12 E-mail address: santofabio.corsino@unipa.it (Santo Fabio Corsino)

26 **Abstract**

27 The integration of one anaerobic reactor in the mainstream (AMSR) of a pre-denitrification-MBR  
28 was evaluated with the aim to achieve simultaneous sludge minimization and phosphorous removal.  
29 The excess sludge production was reduced by 64% when the AMSR was operated under 8h of  
30 hydraulic retention time (HRT). The highest nutrients removal performances referred to organic  
31 carbon (98%), nitrogen (90%) and phosphorous (97%) were obtained under 8 h of HRT. In contrast,  
32 prolonged anaerobic-endogenous conditions were found to be detrimental for all nutrients removal  
33 performances. Similarly, the lowest membrane fouling tendency ( $FR=0.65 \cdot 10^{11} \text{ m}^{-1} \text{ d}^{-1}$ ) was achieved  
34 under 8 h of HRT, whereas it significantly increased under higher HRT. The highest polyphosphate  
35 accumulating organisms kinetics were achieved under HRT of 8 h, showing very high exogenous P-  
36 release ( $46.67 \text{ mgPO}_4\text{-P gVSS}^{-1} \text{ h}^{-1}$ ) and P-uptake rates ( $48.6 \text{ mgPO}_4\text{-P gVSS}^{-1} \text{ h}^{-1}$ ), as well as a not  
37 negligible P-release rate under endogenous conditions at low COD/P ratio ( $\approx 1$ ).

38

39 **Keywords:** Biological nutrients removal; Endogenous P-release; Membrane BioReactor; Membrane  
40 fouling; Sludge minimization.

41

42

43

44

45

46

47

48

49

50

- 51 **List of abbreviations and symbols**
- 52 AMSR – Anaerobic Main Stream Reactor
- 53 MBR – Membrane BioReactor
- 54 HRT – Hydraulic Retention Time
- 55 FR – Fouling Rate
- 56 PAO – Polyphosphate Accumulating Organisms
- 57 SRT – Sludge Retention Time
- 58 BNR – Biological Nutrient Removal
- 59 CAS – Conventional Activated Sludge
- 60 OSA – Oxidic Settling Anaerobic
- 61 SRR – Sludge Retention Reactor
- 62 RAS - Return Activated Sludge
- 63 EPS – Extracellular Polymeric Substances
- 64 SMP – Soluble Microbial Products
- 65 ASSR – Anaerobic Side-Stream Reactor
- 66 OHO – Ordinary Heterotrophic Organisms
- 67 TSS –Total Suspended Solid
- 68 VSS – Volatile Suspended Solid
- 69 SCOD – Soluble Chemical Oxygen Demand
- 70 COD – Chemical Oxygen Demand
- 71 CIP – Clean In Place
- 72 DO - Dissolved Oxygen (DO)
- 73 ORP – Oxidation Reduction Potential
- 74 UCT – University of Cape Town
- 75 F/M – Food/Microorganisms
- 76 EBPR – Enhanced Biological Nutrient Removal

- 77 TN – Total Nitrogen
- 78 TP – Total Phosphorous
- 79  $R_t$  – Total Resistance
- 80 PN – Proteins
- 81 PS – Polysaccharides
- 82 PDVF – Polyvinylidene fluoride
- 83 RIS – Resistance In Series
- 84  $Y_{sto}$  – Storage yield coefficient
- 85  $Y_H$  – Maximum heterotrophic yield coefficient
- 86  $Y_{obs}$  – Observed yield coefficient
- 87  $f_{XH}$  – Active fraction of the ordinary heterotrophic biomass
- 88  $b_H$  – Endogenous decay coefficient of the ordinary heterotrophic biomass
- 89  $\mu_H$  – Net growth coefficient of the ordinary heterotrophic biomass
- 90
- 91

92 **Introduction**

93 The advanced technologies for wastewater treatment based on biological processes are aimed to  
94 increase the biological nutrient removal (BNR) performance, while saving energy and minimizing  
95 the excess sludge production (Moreira et al., 2015; Ioannou-Ttofa et al., 2016; Semblante et al.,  
96 2016a).

97 Among the new and advanced technologies that have been developed with this aim, the membrane  
98 bioreactor (MBR), the moving bed biofilm reactor (MBBR), the aerobic granular sludge (alias  
99 Nereda<sup>®</sup>) are considered the most promising to attain this goal (Pronk et al., 2015). In these systems,  
100 nutrients removal significantly improve due to the increase of biomass retention, thus enhancing the  
101 plants' loading capacity. Moreover, due to the higher value of the sludge retention time (SRT), low  
102 waste-sludge production could be achieved. Indeed, the selection of slow growing microorganisms  
103 promotes low sludge yields (Troiani et al., 2011; Devlin et al., 2016).

104 Nevertheless, similar results could be achieved by retrofitting existing plants based on conventional  
105 biological technologies, i.e., conventional activated sludge (CAS) systems. For instance, the oxic-  
106 settling-anaerobic (OSA) process, featuring the modification of a CAS plant by placing an anaerobic  
107 sludge retention reactor (SRR) in the return activated sludge (RAS) flow, represents one of the most  
108 potentially cost-effective and low impact solution to achieve excess sludge minimization (Foladori et  
109 al., 2010).

110 Several biological mechanisms contribute to the excess sludge reduction (even simultaneously).  
111 Among these, the biological maintenance metabolism, the uncoupling metabolism, the extracellular  
112 polymeric substances (EPS) destruction, the bacteria predation, have been highly debated in previous  
113 literature. (Wang et al., 2013). Moreover, many studies states that the sludge alternation between  
114 feasting and fasting conditions under anaerobic and aerobic environments, could be favorable to the  
115 development of polyphosphate accumulating organisms (PAO) (Goel and Noguera, 2006; Datta et  
116 al., 2009).

117 The excess sludge minimization in MBR systems was thoroughly investigated in anaerobic side-  
118 stream reactor (ASSR) configuration, consisting in the placement of one anaerobic reactor in the RAS  
119 line of the MBR plant (Kim et al., 2012; Semblante et al., 2014, 2016a). Although the majority of the  
120 studies reported excellent results towards sludge minimization, a collateral issue that arises might be  
121 represented by a long-term worsening of membrane permeability. Indeed, a worsening of the  
122 microbial cells features, including the production of EPS and the increase of soluble microbial  
123 products (SMP) in the bulk liquid deriving from the cellular lysis, might enhance the membrane  
124 fouling (in this case also referred to as “biofouling”) (Wang et al., 2013).

125 Recently, a novel layout for MBR system was proposed with the aim to achieve excess sludge  
126 minimization by applying the anaerobic mainstream reactor (AMSR) configuration, while preserving  
127 the membrane permeability (de Oliveira et al., 2018). de Oliveira and co-workers proposed a  
128 modification of the conventional pre-denitrification scheme, by placing one anaerobic reactor in the  
129 mainstream between the anoxic and the aerobic reactor. In this system, a portion of the activated  
130 sludge flow from the anoxic reactor was fed to the anaerobic SRR and subsequently to the aerobic  
131 reactor. In the SRR, because of the anaerobic starvation, uncoupling metabolism occurred, thereby  
132 favoring the achievement of low biomass yield (Semblante et al, 2016a). de Oliveira and co-workers  
133 compared the ASSR configuration with the AMSR one and demonstrated that approximately 30% of  
134 excess sludge minimization could be achieved operating with 6 hours of hydraulic retention time  
135 (HRT) in the anaerobic reactor. Nonetheless, the authors suggested that an increase in the HRT could  
136 be beneficial to achieve higher excess sludge reduction. Moreover, the authors observed that in the  
137 AMSR configuration a significant increase of nutrients removal was obtained, thus suggesting the  
138 feasibility to achieve significant biological phosphorous removal. However, because in the AMSR  
139 configuration the anaerobic tank is placed downstream the anoxic reactor, where the rapidly  
140 biodegradable carbon was already depleted for denitrification, phosphorous release by PAOs would  
141 occur under endogenous conditions because of the low availability of residual carbon source, in  
142 contrast with what generally observed in conventional BNR plants (Zuthi et al., 2013).

143 In this light, this study was aimed at evaluating the effects of different HRTs in the anaerobic reactor  
144 of a AMSR-MBR plant in terms of simultaneous achievement of sludge minimization and biological  
145 phosphorous removal. Moreover, insights about the ordinary heterotrophic organisms (OHO) and  
146 PAO kinetics, as well as the membrane-fouling tendency were provided.

147

## 148 **Materials and methods**

### 149 *2.1 Pilot plant configuration*

150 The experimental campaign was carried out on a MBR pilot plant operating at room temperature ( $20$   
151  $\pm 6$  °C). The MBR pilot plant layout was realized according to a pre-denitrification scheme, consisting  
152 of one anoxic reactor followed by one aerobic, each characterized by a volume of 22.5 L. Further  
153 details about the plant configuration can be found in literature (de Oliveira et al., 2018).

154 Subsequently, the pre-denitrification scheme was modified by placing a sludge retention reactor,  
155 operated under anaerobic conditions, between the anoxic and the aerobic ones. This configuration  
156 was referred to as anaerobic mainstream reactor (AMSR). A portion of the activated sludge flow from  
157 the anoxic reactor was fed to the anaerobic reactor (continuously mixed by a mechanical stirrer) with  
158 a flow rate almost equal to the influent one ( $4.32 \text{ L h}^{-1}$ ) and then fed to the aerobic reactor. Different  
159 HRTs in the anaerobic reactor were investigated during the experiments. In detail, HRTs of 6 h, 8 h  
160 and 10 h were imposed by increasing the reactor volume, while maintaining the same influent flow  
161 coming from the anoxic reactor.

162

### 163 *2.2 Experimental set-up*

164 The MBR plant was seeded with activated sludge collected from a municipal WWTP characterized  
165 by a conventional activated sludge scheme (inoculum sludge concentration:  $6.15 \text{ gTSS L}^{-1}$ ) and it  
166 was fed with synthetic wastewater. The composition of the synthetic wastewater is reported as  
167 supplementary information (SI). The experimental campaign had a duration of 198 days and it was

168 divided into four periods, namely: Period 1 (56 days), Period 2 (49 days), Period 3 (49 days) and  
 169 Period 4 (44 days). Specifically, during Period 1 the MBR operated with the conventional pre-  
 170 denitrification scheme, until steady conditions were achieved. During the first 21 days of Period 1 the  
 171 sludge retention time (SRT) was not controlled and no dedicated sludge wasting operations were  
 172 carried out. The aim was to enable the activated sludge adaptation to the synthetic medium and the  
 173 new plant configuration. To avoid the activated sludge ageing, during the remaining 35 days of Period  
 174 1, a known amount of sludge was withdrawn daily, including the samples for physical-chemical  
 175 analyses, with the aim to maintain a SRT close to 35-40 days. The same SRT was imposed during the  
 176 following experimental periods. The excess sludge production was evaluated in terms of observed  
 177 heterotrophic growth yield ( $Y_{obs}$ ) and the  $Y_{obs}$  obtained in Period 1 was assumed as the reference  
 178 value to evaluate the sludge minimization efficiency achieved in the following experimental periods.  
 179 In Period 2 the MBR was operated with AMSR configuration for 49 days with a HRT in the anaerobic  
 180 reactor of 6 h. When a steady-state excess sludge production was achieved, the HRT was increased  
 181 to 8 h and 10 h in Period 3 and Period 4, respectively. Because of the relatively high SRT value, the  
 182 achievement of steady state conditions in each periods was evaluated based on the biological  
 183 performances, kinetic parameters and excess sludge production, instead of considering a duration of  
 184 three times SRT.

185 Table 1 summarizes the main operating conditions and the average characteristics of the influent  
 186 wastewater throughout experiments.

187 **Table 1:** Summary of the wastewater characteristics and the main operating conditions of the MBR

Parameter	Unit	Period 1	Period 2	Period 3	Period 4
		Value	Value	Value	Value
Soluble COD (SCOD)	[mg L <sup>-1</sup> ]	440±18	477±21	566±13	571±15
Ammonium nitrogen (TN)	[mg L <sup>-1</sup> ]	41±3	40±5	41±4	43±3
Total phosphorous (TP)	[mg L <sup>-1</sup> ]	11.8±1.6	12.4±1.3	11.5±0.8	11.0±0.9
Influent flow rate	[L h <sup>-1</sup> ]	2.4	2.4	2.4	2.4
Food to microorganism (F/M)	[kgCOD kgTSSd <sup>-1</sup> ]	0.08±0.02	0.08±0.01	0.09±0.02	0.12±0.01
SRT	[d]	∞ - 35/40	35/40	35/40	35/40
Total plant HRT	[h]	18.75	24.6	24.6	24.6
Volume of AMSR	[L]	-	14.4	19.2	24
AMSR HRT	[h]	-	6	8	10
Period duration	[d]	56	49	49	44



188 *2.3 Analytical methods and activated sludge characterization*

189 All the chemical-physical analyses including total and volatile suspended solid (TSS, VSS)  
190 concentrations, soluble chemical oxygen demand (SCOD), ammonium nitrogen (NH<sub>4</sub>-N), nitrate  
191 nitrogen (NO<sub>3</sub>-N), nitrite nitrogen (NO<sub>2</sub>-N) and orthophosphate (PO<sub>4</sub>-P) were performed according  
192 to standard methods (APHA, 2005). The chemical oxygen demand (COD), NH<sub>4</sub>-N, NO<sub>3</sub>-N, NO<sub>2</sub>-N  
193 and PO<sub>4</sub>-P were measured in the influent, in the supernatant of the mixed liquor from each reactor  
194 and in the clean-in-place (CIP) tank. Briefly, the aim of CIP tank was to store a portion of permeate  
195 for the membrane ordinary backwashing. TSS and VSS were measured in the mixed liquor of all the  
196 reactors. Dissolved oxygen (DO) concentration, oxidation-reduction potential (ORP) and pH were  
197 measured in all the reactors by means of specific probes (WTW 3310).

198 The EPS and SMP were extracted from the activated sludge according to the literature (Le-Clech et  
199 al., 2006). For each fraction, the polysaccharides and protein concentrations were determined  
200 according to the phenol-sulphuric acid method (DuBois et al., 1956) and by the Folin method (Lowry  
201 et al., 1951), respectively.

202 With the aim to give an insight to the membrane fouling mechanisms, specific measurements on the  
203 cake layer were performed. In particular, after the cake was manually removed, the amount and  
204 composition of EPS was evaluated according to the above reported method, as well as the relative  
205 hydrophobicity (Rosenberg, 1984).

206  
207 *2.4 Assessment of biomass growth and heterotrophic kinetics parameters*

208 The  $Y_{obs}$  was calculated through a mass balance according to literature (de Oliveira et al., 2018). The  
209 evaluation of the heterotrophic kinetic parameters, including the endogenous decay coefficient ( $b_H$ ),  
210 the net growth coefficient ( $\mu_H$ ), the maximum yield coefficient ( $Y_H$ ) and the active fraction of the  
211 ordinary heterotrophic biomass ( $f_{XH}$ ), was carried out at controlled temperature ( $20 \pm 0.1$  °C)  
212 according to the literature (Capodici et al., 2016). The calculations of the above mentioned parameters  
213 are reported as supplementary information (SI).

214 Moreover, specific batch tests aimed at assessing the PAO kinetics in terms of phosphate release and  
215 uptake rates were carried out at the end of each experimental period. More precisely, these tests were  
216 performed in batch reactors (1.5 L) at controlled temperature ( $20 \pm 0.1$  °C). A known volume of  
217 mixed liquor was withdrawn from the anoxic reactor and put in the batch reactor where it was diluted  
218 with the permeate in order to obtain a TSS concentration of approximately  $3 \text{ gTSS L}^{-1}$  ( $2.1 \text{ gVSS L}^{-1}$ ).  
219 The sample was continuously mixed through a magnetic stirrer.

220 The sample was maintained under endogenous conditions until nitrates, if present, were completely  
221 depleted. At this point, a known amount of sodium acetate was added, in order to obtain a COD  
222 concentration of approximately  $200 \pm 20 \text{ mg L}^{-1}$ . The ORP was continuously monitored in order to  
223 ensure the achievement of anaerobic conditions (ORP  $< -150 \text{ mV}$ ). Subsequently, samples were taken  
224 at regular time intervals (15-20 minutes) and  $\text{PO}_4\text{-P}$  and COD were measured after samples filtration  
225 through a  $0.45 \mu\text{m}$  membrane. Sampling was stopped when the phosphate release reached its  
226 maximum value. Hereafter, the batch reactor was aerated and the oxygen concentration was  
227 maintained close to the saturation value ( $9 \text{ mg L}^{-1}$ ). During this phase, phosphate uptake occurred  
228 very rapidly, thus the sampling interval was increased (10 minutes) until all the phosphate  
229 concentration was close to  $1 \text{ mg L}^{-1}$ .

230 The phosphate release rate was calculated in the anaerobic period as the ratio between the variation  
231 of the phosphate concentration and the time interval during which the release occurred. More  
232 precisely, the P-release was calculated both in the presence of external COD (named exogenous P-  
233 release) and in absence of this (named endogenous P-release). The exogenous P-release was  
234 calculated as the release occurred until external COD in the batch reactor was not completely  
235 depleted, whereas the endogenous P-release was measured as the P-release occurred after external  
236 COD was completely depleted.

237

238 *2.5 Membrane fouling analysis*

239 The membrane fouling was investigated by assessing the total resistance to filtration ( $R_T$ ), the fouling  
240 rate (FR) and the specific deposition mechanisms according to a previous study (de Oliveira et al.,  
241 2018). The details about the calculation of  $R_T$ , FR and RIS model application are reported as SI.

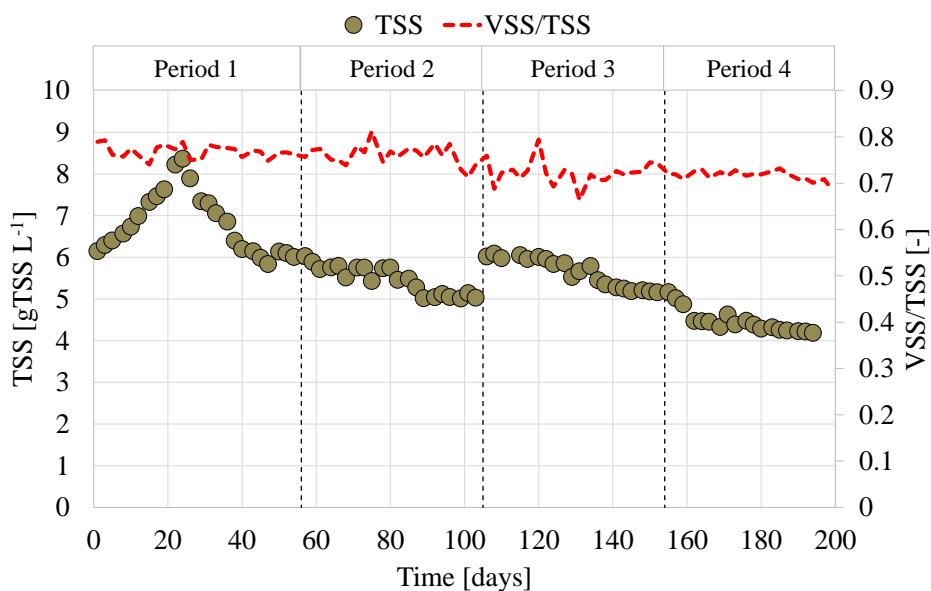
242

243

### 244 3. Results and Discussion

#### 245 3.1 Biomass growth and excess sludge production

246 The trend of TSS concentration as well as the ratio between VSS and TSS throughout experiments  
247 are shown in Figure 1.



248

249 **Figure 1:** Trends of TSS concentration and VSS/TSS ratio during the experiment

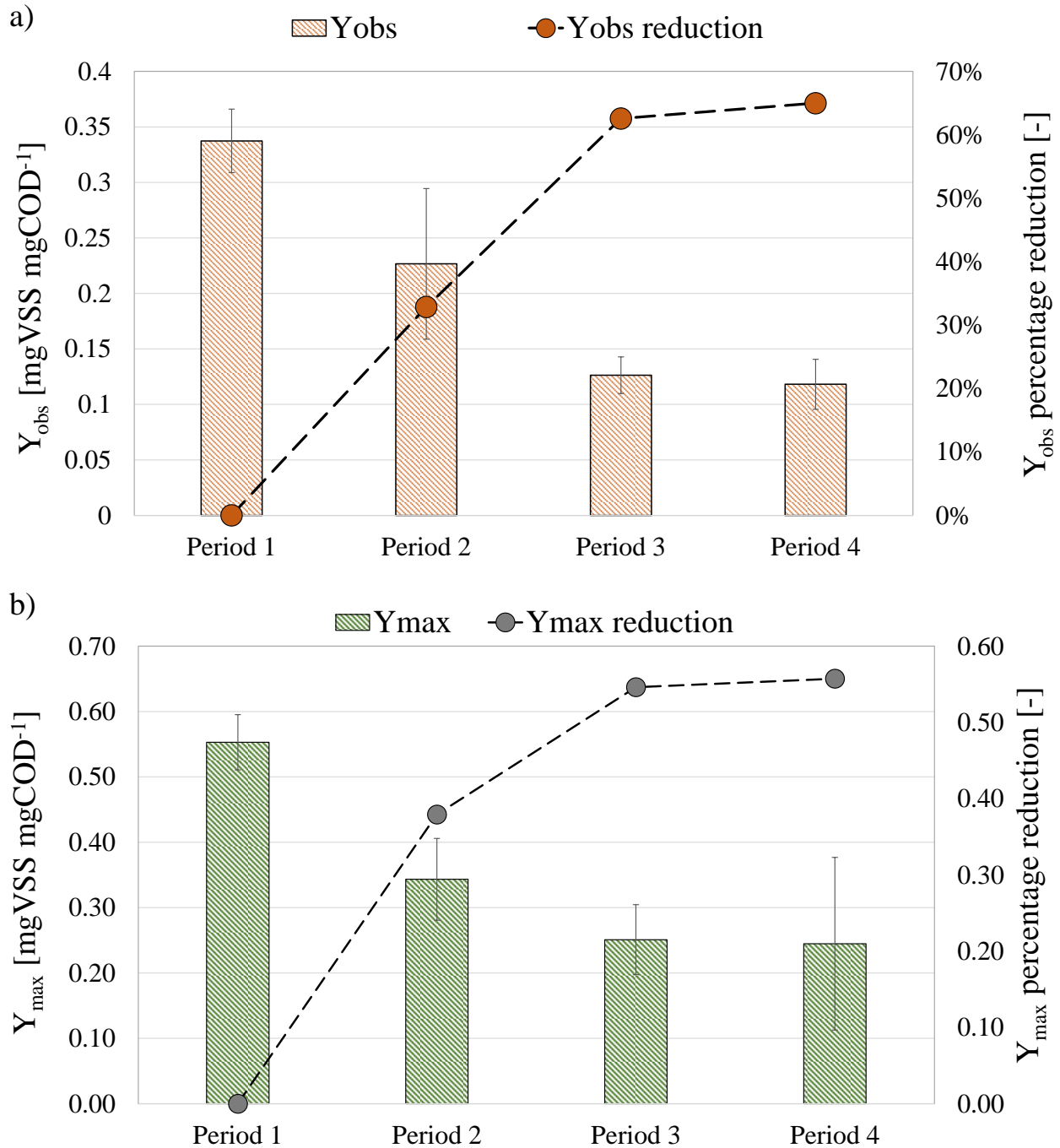
250

251 In Period 1, the TSS concentration increased from 6.15 gTSS L<sup>-1</sup> to a 8.5 gTSS L<sup>-1</sup>, indicating that  
252 the biomass was successfully acclimated to the new operating conditions of the MBR system. When  
253 a regular sludge withdrawn was performed, the TSS concentration decreased reaching an almost  
254 constant value of 6 gTSS L<sup>-1</sup>. In Period 2, the TSS concentration showed a slightly decreasing trend,  
255 reaching a steady value of 5 gTSS L<sup>-1</sup> at the end of this period. At the beginning of Period 3, the TSS

256 concentration was increased to  $6 \text{ gTSS L}^{-1}$  by adding a portion of the sludge wasted in Period 2, in  
257 order to achieve similar conditions of Period 1 in terms of TSS and food/microorganisms (F/M) ratio.  
258 In Period 3, the TSS concentration decreased according to what observed in Period 2, reaching an  
259 almost stable value of  $5.20 \text{ gTSS L}^{-1}$  at the end of the period. Compared to the previous periods, the  
260 decreasing trend observed in Period 3 showed a higher slope, indicating that the higher was the HRT  
261 in the anaerobic reactor the lower was the excess sludge production. This result confirmed that the  
262 integration of the anaerobic reactor in the AMSR scheme involved a decrease in the biomass net  
263 growth, thus favoring a lower excess sludge production. Even in Period 4, the TSS concentration  
264 decreased from  $5.20 \text{ gTSS L}^{-1}$  to  $4.22 \text{ gTSS L}^{-1}$  at the end of the experiments, showing a similar trend  
265 of Period 3.

266 The VSS/TSS ratio showed a slightly decreased trend throughout experiments. Indeed, the VSS/TSS  
267 of the inoculum was close to 0.77, whereas it decreased to approximately 0.73 at the end of the  
268 experiment.

269 The average  $Y_{\text{obs}}$  values, the maximum yield coefficient ( $Y_{\text{H}}$ ), as well as their respective percentage  
270 reductions obtained in each experimental period are depicted in Figure 2.



271

272 **Figure 2:** Average values of the observed yield coefficient ( $Y_{obs}$ ), the maximum yield coefficient

273 ( $Y_{max}$ ) and their respective percentage reduction obtained in the four experimental periods.

274

275 The average value of the  $Y_{obs}$  (Fig. 2a) in Period 1 was close to 0.33 kgVSS kgCOD<sup>-1</sup> that was slightly

276 higher compared with what observed in other MBR systems operated under similar SRT and F/M

277 values (Wang et al., 2013). Nevertheless, the  $Y_{obs}$  was very similar to what observed by de Oliveira

278 et al. (2018), who operated with acetate based synthetic wastewater and prolonged SRT. After the  
279 plant configuration was changed to AMSR (Period 2), the  $Y_{obs}$  decreased to  $0.22 \text{ kgVSS kgCOD}^{-1}$ ,  
280 showing a reduction of 33% compared to Period 1. This result was in good agreement with what  
281 reported by de Oliveira et al. (2018), thus confirming that it is possible to achieve 30% of  $Y_{obs}$   
282 reduction by operating the anaerobic reactor of AMSR configuration at 6 h. When the HRT of the  
283 anaerobic reactor was increased to 8 h (Period 3), the  $Y_{obs}$  decreased to  $0.12 \text{ kgVSS kgCOD}^{-1}$ , thereby  
284 showing an overall decrease of 62% in the excess sludge production. In Period 4, the increase of the  
285 anaerobic reactor HRT did not provide a significant decrease of the sludge minimization. Indeed, the  
286  $Y_{obs}$  was approximately  $0.11 \text{ kgVSS kgCOD}^{-1}$ , which was very close to what achieved in the previous  
287 period. This result highlighted that the increase of the anaerobic reactor HRT from 8 h to 10 h did not  
288 provide any significant advantage in terms of sludge minimization.

289 The  $Y_H$  decreased from the initial value of approximately  $0.55 \text{ kgVSS kgCOD}^{-1}$  (Period 1) to a  
290 minimum value of  $0.22 \text{ kgVSS kgCOD}^{-1}$  obtained in Period 3 and Period 4 (Fig. 2b). As observed  
291 for the  $Y_{obs}$ , the maximum effect in terms of sludge reduction was obtained under an HRT of 8 h,  
292 whereas no significant improvements were achieved under 10 h of HRT. The similar trends and  
293 values observed for both the  $Y_{obs}$  and  $Y_H$  indicated that the operating parameters (i.e. SRT) had a  
294 negligible role on the overall excess sludge minimization. Therefore, sludge reduction was achieved  
295 because of the change in the plant configuration.

296 The results indicated that the integration of an anaerobic reactor (HRT of 8 h) in the mainstream  
297 enabled 62% of the excess sludge reduction. Compared with a previous study, the AMSR  
298 configuration enabled a slightly lower excess of sludge minimization compared with the ASSR (62  
299 vs 72%) even operating at higher HRT (8 h vs 6 h) (de Oliveira et al., 2018). Nevertheless, it is worth  
300 mentioning that in the present study, the SRT was significantly lower (35-40 d vs infinite SRT),  
301 whereby the contribution of the decay phenomena to the excess sludge minimization was certainly  
302 lower. While comparing the above results with others obtained under controlled SRT (63 days) in  
303 ASSR configuration, it was noted that  $Y_{obs}$  was similar with that observed in the AMSR configuration

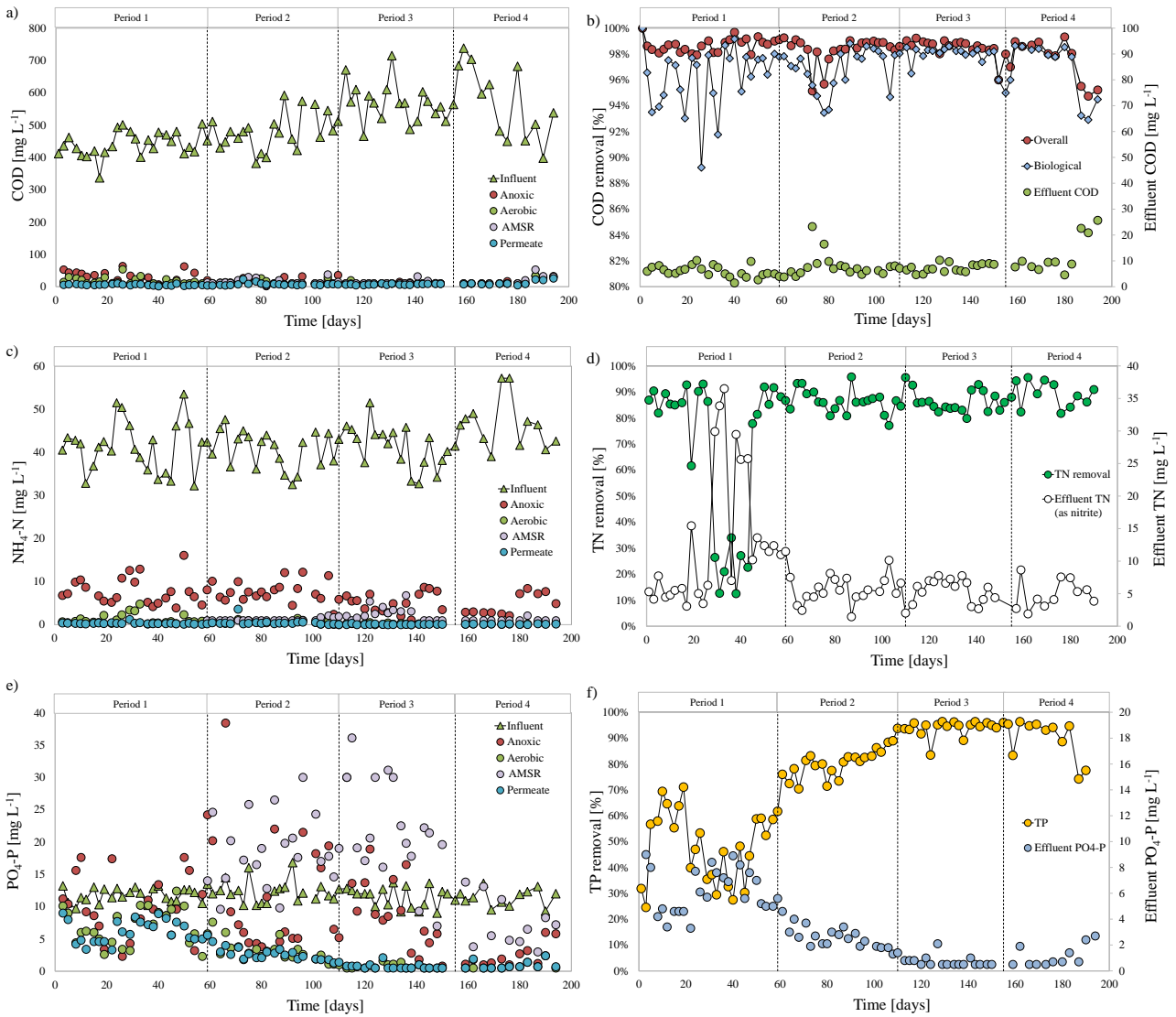
304 (0.12 vs 0.13 kgVSS kgCOD<sup>-1</sup>) but under lower HRT (8 h vs 10 h) (Kim et al., 2012). Similarly, 35%  
305 of sludge reduction was obtained in a SBR connected to an anaerobic side stream reactor operating  
306 under 12 h of HRT and 30 days of SRT (Semblante et al., 2016b). In another study carried out with  
307 ASSR-MBR systems, the maximum excess sludge reduction (55-58%) was achieved under 10-11 h  
308 of HRT in the anaerobic reactor (Saby et al., 2003; Ferrentino et al., 2016). Similarly, Cheng et al.  
309 (2017) observed that the sludge yield decreased by approximately 49.7% in a ASSR-MBR system  
310 with HRT of 5 h in the anaerobic reactor, whereas Coma et al. (2015) obtained a sludge reduction of  
311 18% operating in a University of Cape Town (UCT) system coupled to an anaerobic side stream  
312 reactor under a HRT of 5.9 h.

313 The results obtained in the present study suggested that in general the AMSR configuration might  
314 enable a higher sludge minimization than the ASSR under similar HRT and SRT.

315

### 316 *3.2 Nutrient removal performances*

317 The MBR plant was periodically monitored to evaluate the COD, nitrogen and phosphorous removal  
318 performances (Fig. 3).



319

320 **Fig. 3:** Trends of the COD concentration in the influent, in the supernatant of the anoxic, aerobic  
 321 and AMSR and in the permeate (a); biological and overall COD removal efficiency and effluent  
 322 COD concentration (b); ammonia nitrogen in the influent and in the supernatant of each reactor (c);  
 323 TN removal efficiency and TN concentration (as nitrate) in the permeate (d); PO<sub>4</sub>-P concentration  
 324 in the influent, in the supernatant of each reactor (e); TP removal efficiency and PO<sub>4</sub>-P  
 325 concentration in the permeate.

326

327 In particular, Fig. 3a shows the COD trend in the influent and in the supernatant of each reactor,  
 328 whereas Fig. 3b depicts the overall removal of COD including membrane filtration, as well as the  
 329 COD concentration in the permeate. The influent COD concentration ranged from 80 to 680 mg L<sup>-1</sup>



330 in order to maintain a stable F/M ratio according to the TSS variation and the volume increase of the  
331 system related to the HRT variation in the anaerobic reactor.

332 In Period 1, the COD concentration in the supernatant of the anoxic reactor was close to  $18 \text{ mg L}^{-1}$   
333 (average value) and it slightly decreased after the change of plant configuration, likely due to a more  
334 effective use of the organic carbon for denitrification (Capodici et al., 2015). In contrast, the COD  
335 concentration remained constant when the HRT was increased in Periods 2-4. The COD concentration  
336 in the supernatant of the aerobic reactor decreased during experiments from approximately  $17 \text{ mg L}^{-1}$   
337 (average value in Period 1) to  $10 \text{ mg L}^{-1}$  (average value in Period 3), whereas it increased up to  $19$   
338  $\text{mg L}^{-1}$  in Period 4 (average value), showing an increasing trend with the HRT of the anaerobic  
339 reactor. Similarly, the COD in the supernatant of the anaerobic reactor increased with the HRT,  
340 reaching a maximum value of approximately  $28.9 \text{ mg L}^{-1}$  in Period 4. These results suggest the  
341 occurrence of bacterial lysis in the anaerobic reactor under prolonged HRT. Nevertheless, it is worth  
342 mentioning that the released COD was subsequently degraded in the anaerobic reactor, thus  
343 suggesting the biodegradability of COD generated in the anaerobic reactor, causing a negligible  
344 impact on the overall COD removal efficiency.

345 Referring to COD removal, in Period 1 the removal efficiency due to the biological process gradually  
346 increased suggesting the acclimation of the biomass to the new operational conditions (Fig. 3b). In  
347 Period 2, after the startup of the AMSR configuration, the biological contribution to COD removal  
348 slightly decreased from 98% to approximately 93%. Nevertheless, it was gradually recovered,  
349 reaching a stable value of 98% at the end of Period 2. In Period 3, the biological COD removal stably  
350 close to 96%, showing a slight decrease in the last days of operation. From Period 1 to Period 3, the  
351 overall COD removal was on average equal to 97%, without any significant variation with the change  
352 of plant configuration as well as the HRT increase in the anaerobic reactor. This result confirmed the  
353 high MBR robustness, enabling high COD removal even in presence of temporary decreases of  
354 biological contribution towards COD removal. In contrast, in Period 4 both the biological and the

355 membrane removal efficiencies decreased in the long-term, suggesting that extended HRT values  
356 (higher than 8 h) in the anaerobic reactor could be detrimental in terms of effluent quality.

357 The above results were in good agreement with previous literature, indicating that the released COD  
358 in the anaerobic reactor increased with the HRT (Cheng et al., 2017). Although previous studies  
359 reported that the implementation of the anaerobic reactor improved the COD removal efficiency  
360 (Saby et al., 2003; Semblante et al., 2014), the findings of the present study demonstrated that the  
361 COD removal efficiency decreased with HRT higher than 8 h, in good agreement with what reported  
362 by Ye et al. (2008). It is possible to speculate that under prolonged anaerobic condition, the decrease  
363 of biomass activity was so severe that bacteria resulted unable to cope with the COD release that  
364 occurred in the anaerobic reactor.

365 The trends ammonium concentration in the influent and in the supernatant of each reactor are shown  
366 in Fig. 3c. The average ammonium concentration in the anoxic reactor was approximately equal to  
367  $10 \text{ mg L}^{-1}$  throughout experiments, thus indicating that the ammonium removed for heterotrophic  
368 synthesis accounted for approximately the 64% of the total nitrogen removal. The ammonium  
369 concentration in the supernatant of the aerobic reactor was always lower than  $1 \text{ mg L}^{-1}$ , indicating  
370 that complete nitrification occurred throughout experiments. In the anaerobic reactor a slightly  
371 increase in the ammonium concentration occurred only during Period 3, whereas no significant  
372 variations were observed in the other periods.

373 The main nitrogen form in the permeate was represented by nitrates (Fig. 3d), accounting for more  
374 than 98% of the total nitrogen in the effluent, whereas nitrites were not detected during the entire  
375 experiments duration. In the first two weeks of Period 1, the nitrate concentration in the effluent  
376 increased up to a maximum value of  $36 \text{ mg L}^{-1}$  (38<sup>th</sup> day), whereas it decreased to  $12 \text{ mg L}^{-1}$  at the  
377 end of Period 1, indicating the achievement of steady state conditions. The TN removal efficiency at  
378 steady state was close to 85%. In Period 2, the nitrate concentration in the permeate decreased by  
379 50%, reaching a stable value of  $5 \text{ mg L}^{-1}$  (average value) until the end of the experimental campaign.

380 Accordingly, the TN removal efficiency increased from 86% to 91% after the implementation of the  
381 anaerobic reactor, but no significant improvements were observed with the HRT increase. The  
382 obtained results were in good agreement with previous literature (Semblante et al., 2014; de Oliveira  
383 et al., 2018), indicating that the AMSR configuration enabled a significant improvement of nitrogen  
384 removal efficiency.

385 The trend of orthophosphate concentrations in the supernatant of each reactor are depicted in Figure  
386 3e, while Figure 3f shows the removal efficiency. In Period 1, a slight increase of the phosphorous  
387 concentration in the supernatant of the anoxic reactor was periodically observed, suggesting that  
388 anaerobic condition occasionally occurred likely due to denitrification depletion. Indeed, the P-  
389 release in the anoxic reactor occurred when the TN removal efficiency was close to 90% in Period 1.  
390 In general, in Period 1 the average TP removal efficiency was almost equal to 50%. In Period 2, a  
391 significant release of phosphorous was observed in the anaerobic reactor. Indeed, the average  
392 concentration of orthophosphate in the supernatant of the anaerobic reactor was 20 mg L<sup>-1</sup>, whereas  
393 it was significantly lower in the aerobic reactor (3.28 mg L<sup>-1</sup>) indicating that the integration of the  
394 anaerobic reactor in the mainstream enhanced the orthophosphate release and uptake by PAO  
395 bacteria. Similarly, in Period 3 the PO<sub>4</sub>-P concentration in the anaerobic reactor slightly increased to  
396 25 mg L<sup>-1</sup>, while in the aerobic reactor it decreased to 0.76 mg L<sup>-1</sup>, highlighting a further increase of  
397 TP removal. As noticeable from Fig. 3f, the average TP removal efficiency in Period 2 was close to  
398 78%, showing an increasing trend, whereas it significantly increased in Period 3 reaching a maximum  
399 steady state value of 97%. In Period 4, a significantly lower release of orthophosphates was observed  
400 in the anaerobic reactor, where the average PO<sub>4</sub>-P concentration was of approximately 7 mg L<sup>-1</sup>,  
401 which was slightly higher than that measured in the anoxic reactor (5 mg L<sup>-1</sup>). Overall, the TP removal  
402 efficiency was higher than 90%, on average, while showing a decreasing trend at the end of the  
403 experiment.

404 The above results demonstrated that the change of plant configuration enabled the achievement of  
405 high TP removal performances. In the anaerobic reactor, similar conditions in terms of ORP (< -350

406 mV) compared to that of EBPR systems occurred (Chudoba et al., 1992). In previous literature, it was  
407 observed that the integration of one anaerobic reactor in the plant layout (i.e. OSA process), promoted  
408 the selection of PAO (Semblante et al., 2014). However, some contradictory results in terms of  
409 phosphorus removal were found in these systems. Among these, Ye et al. (2008) observed that TP  
410 removal efficiency increased from 48% to 58% in a CAS-OSA system, whereas Saby et al. (2003)  
411 reported that TP removal in a MBR-OSA decreased from 55% to 28% when the ORP in the anaerobic  
412 reactor was adjusted to -250 mV. Moreover, Velho et al. (2016) observed that coupling an ASSR in  
413 a UCT scheme had negative effects on phosphorous removal. Velho and co-authors emphasized that  
414 the main drawback affecting phosphorus removal in ASSR configuration was the huge release of  
415 orthophosphate under prolonged anaerobic conditions ( $ORP < -250$  mV), imposed to maximize the  
416 excess sludge minimization.

417 In the AMSR configuration, significant differences compared to a conventional EBPR system can be  
418 found. Indeed, the COD/P ratio in the AMSR, close to 1:1, was significantly lower than that  
419 commonly observed in EBPR systems ( $> 20:1$ ). Moreover, in a conventional EBPR system  
420 phosphorous is separated from wastewater through the disposal of waste sludge enriched in  
421 orthophosphate, whereas in the AMSR system the achievement of sludge minimization reduced the  
422 amount of sludge to be withdrawn, thus leading to a potential accumulation of  $PO_4$ -P within the  
423 system.

424 The results obtained in the present study demonstrated that very high TP removal efficiencies were  
425 achieved in the AMSR configuration, although the low COD/P ratio and the low amount of sludge  
426 withdrawn. This result suggested that a different mechanism of phosphorous removal occurred in the  
427 AMSR system, which favored the simultaneous achievement of P-removal and sludge minimization.

428

### 429 *3.3 Behavior of OHO and PAOs kinetics*

430 The main biokinetics parameters of OHO are summarized in Table 2.

431

**Table 2:** Summary of the main biokinetics parameters of the OHO.

Parameter	Unit	Period 1	Period 2	Period 3	Period 4
Maximum heterotrophic growth rate ( $\mu_{\max,H}$ )	[d <sup>-1</sup> ]	2.512±0.131	1.426±0.093	1.190±0.078	1.230±0.025
Endogenous decay coefficient ( $b_H$ )	[d <sup>-1</sup> ]	0.109±0.246	0.157±0.104	0.287±0.086	0.291±0.046
Heterotrophic active biomass ( $f_{XH}$ )	[%]	13.80±0.4%	3.74±0.2%	3.40±0.2%	1.14±0.16%
Specific Oxygen Uptake Rate (SOUR)	[mgO <sub>2</sub> L <sup>-1</sup> h <sup>-1</sup> ]	30.46±11.2	30.82±4.6	31.73±5.2	40.31±3.6
Storage Yield Coefficient ( $Y_{sto}$ )	[mgCOD mgCOD <sup>-1</sup> ]	0.57±0.12	0.67±0.15	0.69±0.09	0.63±0.08

432

433 The maximum heterotrophic growth rate ( $\mu_{\max,H}$ ) significantly decreased from 2.51 d<sup>-1</sup> to 1.43 d<sup>-1</sup>  
434 from Period 1 to Period 2, thereby indicating a decrease of cell synthesis after the startup of the  
435 AMSR. When the HRT in the AMSR was increased to 8 h (Period 3), the  $\mu_{\max,H}$  slightly decreased to  
436 1.19 d<sup>-1</sup>, whereas it only slightly increased in Period 4 to 1.23 d<sup>-1</sup>. The decrease of the  $\mu_{\max,H}$  suggested  
437 the occurrence of the uncoupling metabolism. Indeed, it is well known that the sludge cycling between  
438 anaerobic and aerobic conditions induces the biomass to use internal energy sources (ATP) for  
439 maintenance metabolism. This causes the detachment of catabolism from anabolism cutting off  
440 energy for cellular propagation. Consequently, the bacterial growth rate decreased by more than 50%  
441 from Period 1 to Period 2. The increase of the anaerobic HRT caused a further decrease (almost 15%)  
442 in Period 3, whereas no significant changes were observed in Period 4 characterized by 10 h of HRT  
443 in the anaerobic compartment.

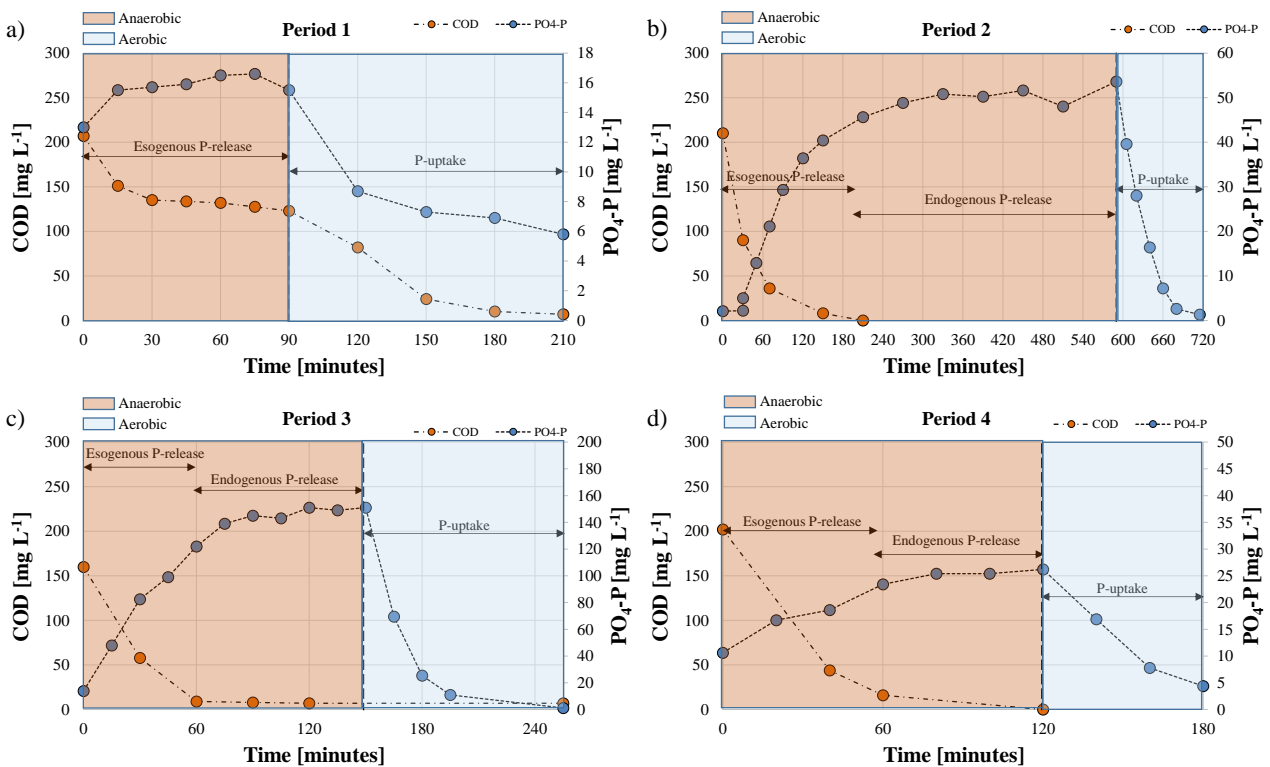
444 The endogenous decay coefficient ( $b_H$ ) increased according to the HRT increase in the AMSR. The  
445 endogenous decay coefficient increased by approximately 50% when the AMSR configuration was  
446 implemented (Period 2), whereas it almost doubled in Period 3. The maximum value of the  $b_H$  was  
447 observed in Period 4 (0.291 d<sup>-1</sup>), although it not significantly increased when the HRT was extended  
448 from 8 h to 10 h. The increase of  $b_H$  could be related to the intensifying of decay phenomena, thus  
449 confirming that under extended substrate-limitation conditions, the biomass decay and cryptic growth  
450 mechanisms were favored.

451 Based on the above results, it can be concluded that the contribution of the uncoupling metabolism  
452 to the excess sludge reduction was maximum in Period 2 and it was not significantly affected by the  
453 HRT increase in the anaerobic reactor. In contrast, the contribution of decay phenomena and cryptic  
454 growth increased with the anaerobic HRT, although showing a not linear relationship at HRT higher  
455 than 8 h. The net growth rate, evaluated as the difference between  $\mu_{\max,H}$  and  $b_H$ , resulted minimum  
456 in Period 3, when the AMSR operated under HRT of 8 h. This finding was in good agreement with  
457 the results above discussed, confirming that the maximum efficiency in terms of sludge minimization  
458 was observed in Period 3.

459 According to the above results, the heterotrophic active fraction ( $f_{XH}$ ) significantly decreased from  
460 Period 1 (13.8%) to Period 2 (3.74%). Hereafter, the  $f_{XH}$  slightly decreased with the HRT increase,  
461 reaching a minimum value of 1.14% in Period 4. This result confirmed that the exposure of biomass  
462 to stressful conditions caused a significant decrease of the bacterial cells synthesis. Moreover, since  
463 the VSS/TSS ratio remained almost constant throughout experiments, a significant accumulation of  
464 endogenous residue occurred likely due to the membrane retention. This aspect, as better outlined in  
465 the following, could have entailed important implications in the phosphorous removal mechanism.

466 The specific oxygen uptake rate (SOUR) slightly increased from Period 1 ( $30 \text{ mgO}_2 \text{ L}^{-1}\text{h}^{-1}$ ) to Period  
467 3 ( $31.7 \text{ mgO}_2 \text{ L}^{-1}\text{h}^{-1}$ ), whereas it significantly arose in Period 4 to approximately  $40 \text{ mgO}_2 \text{ L}^{-1}\text{h}^{-1}$ . The  
468 SOUR increase was previously observed in OSA systems (Semblante et al., 2016b). The sharp  
469 increase of SOUR was likely related to the alternation of fasting/feasting conditions, which led the  
470 starved biomass to use more oxygen when it was returned to the mainstream aerobic reactor where a  
471 high substrate availability was ensured by the influent wastewater. However, in the AMSR layout,  
472 the biomass flowed from the anaerobic to the aerobic reactor where a poor substrate availability  
473 existed. This aspect implied that the alternation of fasting/feasting conditions did not significantly  
474 contribute to the excess sludge reduction at least until Period 3. Nevertheless, in Period 4 the SOUR  
475 significantly increased (+25%) suggesting that the alternation of fasting/feasting conditions likely  
476 occurred in this period. This result was likely due to the increase of the endogenous decay that favored

477 cell lysis phenomena. In this way, the cell lysis in the anaerobic reactor enhanced the availability of  
 478 soluble and particulate substrates, which were used by other bacteria for cryptic growth in the aerobic  
 479 reactor, thereby resulting in the increase of the oxygen depletion rate.  
 480 Lastly, the storage yield coefficient ( $Y_{sto}$ ) that represents the amount of organic substrate converted  
 481 into internal storage products, increased from  $0.57 \text{ mgCOD mgCOD}^{-1}$  to  $0.67 \text{ mgCOD mgCOD}^{-1}$   
 482 after the AMSR was started-up in Period 2. The maximum  $Y_{sto}$  was obtained in Period 3 ( $0.69$   
 483  $\text{mgCOD mgCOD}^{-1}$ ), whereas it slightly decreased in Period 4 ( $0.63 \text{ mgCOD mgCOD}^{-1}$ ) when the  
 484 HRT in the AMSR was increased from 8 h to 10 h. These results indicated that the integration of the  
 485 AMSR was favorable for the growth of bacteria with internal storage ability (i.e., PAO).  
 486 Coupled to the OHO biokinetics evaluation, specific kinetic tests aimed at assessing the PAO kinetic  
 487 behavior were assessed. Figure 4 shows the trends of orthophosphate and COD concentrations during  
 488 the batch tests performed from Period 1 to Period 4.



489

490 **Figure 4:** Results of the kinetic tests carried out in Period 1 (a), Period 2 (b), Period 3 (c) and

491

Period (4).

492 In Period 1, no significant P-release occurred during the anaerobic phase, suggesting a very poor  
493 PAOs activity. In the aerobic phase, a not negligible P-uptake was observed, resulting in a removal  
494 of approximately 50%, according to what previously discussed referring to the TP removal efficiency  
495 observed in Period 1. The P-release occurred in presence of the external carbon source (sodium  
496 acetate) supplied at the beginning of the batch test, resulting in a P-release rate of approximately 0.76  
497  $\text{mgPO}_4\text{-P gVSS}^{-1} \text{h}^{-1}$ , whereas the P-uptake rate was  $2.31 \text{ mgPO}_4\text{-P gVSS}^{-1} \text{h}^{-1}$ . In Period 2, during the  
498 anaerobic phase a significant P-release was observed. More precisely, with the external carbon source  
499 the  $\text{PO}_4\text{-P}$  concentration increased from  $12 \text{ mg L}^{-1}$  to  $48 \text{ mg L}^{-1}$  with a P-release rate of  $5.90 \text{ mgPO}_4\text{-}$   
500  $\text{P gVSS}^{-1} \text{h}^{-1}$ . Interestingly, P-release was still observed even in the absence of the external carbon  
501 source, thereby suggesting that orthophosphate release occurred under endogenous conditions. The  
502 release rate under endogenous conditions was of approximately  $0.6 \text{ mgPO}_4\text{-P gVSS}^{-1} \text{h}^{-1}$ , thus  
503 resulting one order of magnitude lower compared to the exogenous P-release rate. The P-uptake  
504 during the aerobic phase increased up to  $39.7 \text{ mgPO}_4\text{-P gVSS}^{-1} \text{h}^{-1}$ . In Period 3, the exogenous P-  
505 release was of approximately  $18.90 \text{ mgPO}_4\text{-P L}^{-1}\text{h}^{-1}$ , suggesting the achievement of the maximum  
506 activity of PAOs. Even in this case, the P-release under endogenous conditions was observed, with a  
507 release rate of  $3.08 \text{ mgPO}_4\text{-P gVSS}^{-1} \text{h}^{-1}$ . The P-uptake during the aerobic phase was close to  $48.6$   
508  $\text{mgPO}_4\text{-P gVSS}^{-1} \text{h}^{-1}$ , significantly higher compared to the previous period. In Period 4, both the  
509 exogenous and endogenous P-release rates decreased to  $6.10 \text{ mgPO}_4\text{-P gVSS}^{-1} \text{h}^{-1}$  and  $1.33 \text{ mgPO}_4\text{-P}$   
510  $\text{gVSS}^{-1} \text{h}^{-1}$ , respectively. Also the P-uptake during the aerobic phase that decreased to  $10.38 \text{ mgPO}_4\text{-}$   
511  $\text{P gVSS}^{-1} \text{h}^{-1}$ .

512 The obtained results were in good agreement with the TP removal performances previously discussed.  
513 Both the exogenous and the endogenous P-releases and P-uptake increased with the HRT of the  
514 AMSR reaching a maximum value at 8 h of HRT.

515 Comparing the P-release and P-uptake rates obtained in this study with those reported in the literature,  
516 it can be stated that the exogenous P-release was very good in Period 3 (P-release  $> 7 \text{ mgPO}_4\text{-P gVSS}$   
517  $\text{h}^{-1}$ ), whereas it was good in Period 2 and Period 4 (P-release =  $3\div 7 \text{ mgPO}_4\text{-P gVSS}^{-1} \text{h}^{-1}$ ), according



518 to the classification proposed by Janssen, (2002). Similarly, the endogenous P-release was good in  
519 Period 3 ( $3.08 \text{ mgPO}_4\text{-P gVSS}^{-1} \text{ h}^{-1}$ ), whereas it was moderate in Period 2 ( $0.6 \text{ mgPO}_4\text{-P gVSS}^{-1} \text{ h}^{-1}$ )  
520 and Period 4 ( $1.33 \text{ mgPO}_4\text{-P gVSS}^{-1} \text{ h}^{-1}$ ). In contrast, the P-uptake could be defined as very good in  
521 all the periods (P-uptake  $> 7 \text{ mgPO}_4\text{-P gVSS}^{-1} \text{ h}^{-1}$ ), suggesting that the anaerobic P-release was the  
522 limiting process affecting the phosphorous removal process.

523 Our findings demonstrated that phosphorous removal was achieved even under endogenous  
524 conditions, characterized by C/P ratio significantly lower than that of conventional EPBR systems  
525 (Chuang et al., 2011). The mechanism involving phosphorous removal in the AMSR is different  
526 compared to that occurring in conventional EBPR systems. A possible explanation for P removal in  
527 the AMSR-MBR could be that under extended endogenous-anaerobic conditions, bacterial lysis could  
528 result in the release of intracellular substrates that were likely subjected to hydrolysis and  
529 fermentation within the anaerobic reactor. This promoted the formation of simple organic molecules,  
530 which were stored by PAO in intracellular solids such as polyhydroxybutyrate. As aforementioned,  
531 a significant decrease in the heterotrophic active fraction was observed during experiments because  
532 of decay phenomena resulting from AMSR implementation. Nevertheless, the VSS/TSS ratio was  
533 almost constant throughout experiments, thereby suggesting that a significant amount of endogenous  
534 residues, deriving from bacteria decay, was retained within the system by the membrane. The  
535 endogenous residue, constituted by biodegradable organic substances (Ramdani et al., 2012), could  
536 be used as substrate by PAO, thereby proving the carbon source necessary to drive the release of  
537 orthophosphate under anaerobic conditions. Therefore, the membrane provided a crucial contribution  
538 to enable the endogenous residue retention. This would explain the simultaneous achievement of  
539 phosphorous removal and sludge minimization achieved in the AMSR-MBR system.

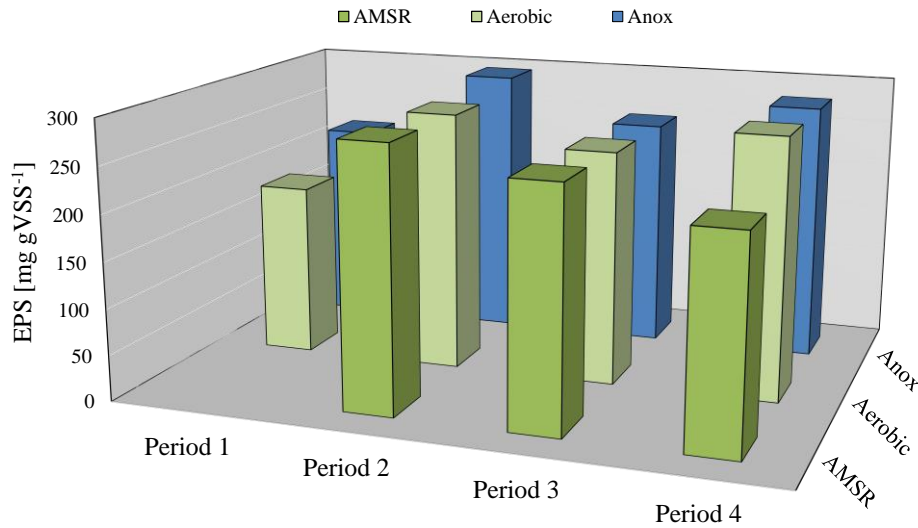
540 The kinetic tests revealed that the HRT of 8 h enabled the highest TP removal efficiency and PAO  
541 biokinetics. Based on the above results, the suggestion is that HRT values in the range of 6-8 h are  
542 favorable for the selection of slow growing microorganisms (i.e., PAO), whereas prolonged anaerobic  
543 conditions in the AMSR might enhance the biomass decay also including PAO bacteria.

544

### 545 3.4 EPS content and composition

546 Previous studies suggested that a possible mechanism leading to sludge reduction in sludge cycling  
547 systems is the destruction of EPS that occurs under anaerobic conditions (Semblante et al., 2014;  
548 Wang et al., 2013). The average EPS content during the experimental periods in the mixed liquor of  
549 each reactor is shown in Figure 5.

550



551

552 **Figure 5:** Average EPS content in the anoxic, aerobic and AMSR during the four experimental  
553 periods

554

555 The average EPSs content in Period 1 was of approximately 200 mgEPS gVSS<sup>-1</sup> and mainly  
556 constituted by the bound fraction that accounted for more than 99% of the entire EPS amount. The  
557 ratio between protein and carbohydrates (PN/PS) was on average close to 6, indicating the  
558 predominance of proteinaceous exopolymers in the EPS matrix. The average EPS content increased  
559 to approximately 290 mgEPS gVSS<sup>-1</sup> in Period 2 and no significant differences were observed among  
560 the anoxic, aerobic and the AMSR reactors. The amount of SMP was negligible (< 2 mgSMP gVSS<sup>-1</sup>

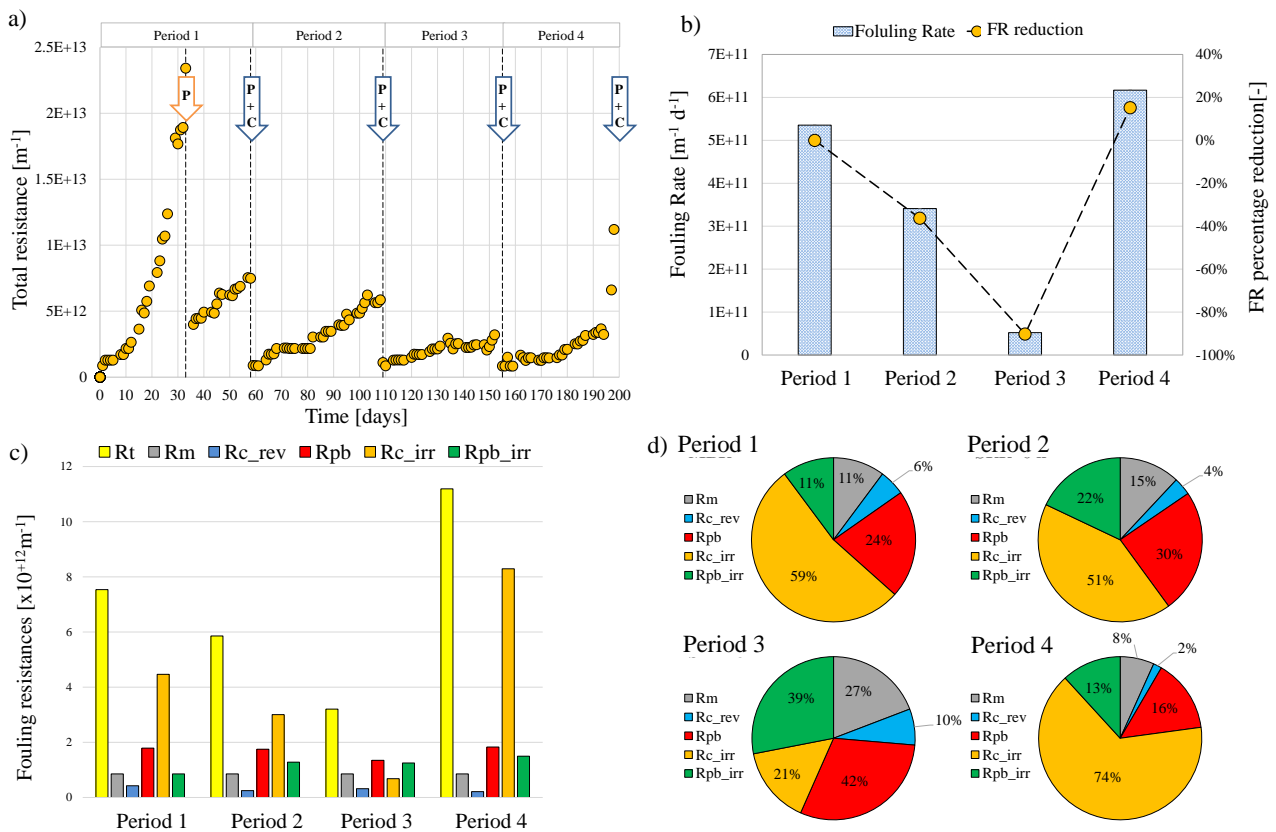
561 <sup>1)</sup> indicating that the no destruction of bound EPS occurred after AMSR implementation in the  
562 original MBR layout in Period 2. The PN/PS ratio increased to 10.7 because a significant decrease in  
563 the carbohydrates (> 40%) amount occurred. In Period 3, the EPS content slightly decreased to  
564 approximately 235 mgEPS gVSS<sup>-1</sup> in all the reactors. As observed during the previous period, the  
565 amount of SMP was negligible, whereas the PN/PS ratio decreased to 5.8, this time because of the  
566 decrease in the protein content (35%). In Period 4, the average EPS content slightly increased to 260  
567 mgEPS gVSS<sup>-1</sup> but in contrast to what observed in the previous periods, the EPS content showed a  
568 20% decrease in the AMSR, indicating that EPS destruction occurred when the HRT in the anaerobic  
569 reactor was higher than 8 h. Nevertheless, no SMP was measured in Period 4 likely due to bacterial  
570 consumption. The PN/PS ratio was similar compared to the previous period (5.7), thereby indicating  
571 that no significant changes in the composition of EPS matrix occurred.

572 Based on the obtained results, a more extensively EPS destruction occurred in Period 4, whereas in  
573 Period 2 and Period 3 only a partial decrease of specific EPS fractions was observed. More precisely,  
574 the amount of carbohydrates slightly decreased under HRT of 6 h, whereas proteins decreased under  
575 a HRT of 8 h. These results were in contrast with that previously reported by de Oliveira et al. (2018),  
576 who observed a significant decrease in the total EPS content when the AMSR (HRT = 6 h) was  
577 implemented in the pre-denitrification MBR layout. Because the only difference between the present  
578 study and that of de Oliveira and co-workers was the SRT (35-40 d vs infinite SRT), it is possible to  
579 speculate that under HRT lower than 8 h, the EPS destruction is mainly driven by prolonged SRT.  
580 On the other hand, under lower SRT values the EPS destruction occurred likely due to prolonged  
581 HRT in the anaerobic reactor (> 8 h). This finding should be taken into account concerning the effects  
582 that EPS destructuration could exert on membrane fouling tendency (Campo et al., 2017).

583

584 *3.5 Membrane fouling analysis*

585 It was previously emphasized that the sludge minimization must not compromise the effluent quality.  
 586 Moreover, in a MBR system also the hydraulic performances of the membrane should be taken into  
 587 account with the aim to optimize the whole process.  
 588 Figure 6 depicts the trend of  $R_T$ , FR as well as the mechanisms involved in the membrane fouling  
 589 mechanism.  
 590



591  
 592 Legend: P: membrane physical cleaning; P+C: membrane physical+chemical cleaning;  $R_t$ : total resistance;  $R_m$ :  
 593 membrane resistance;  $R_{c\_rev}$ : reversible cake resistance;  $R_{pb}$ : pore blocking resistance;  $R_{c\_irr}$ : irreversible cake  
 594 resistance;  $R_{pb\_irr}$ : irremovable pore blocking resistance

595  
 596 **Figure 6:** The trend of the total resistance of the membrane (a), the average fouling rate during the  
 597 four experimental periods (b), the total resistance decomposition (c), and the contribution of each  
 598 fouling mechanism to the overall membrane fouling (d).

599

600 In Period 1, the  $R_T$  increase was characterized by two different trends (Fig. 6a). Indeed, the  $R_T$  rapidly  
601 increased when the MBR was operated under a complete sludge retention strategy, whereas it was  
602 characterized by a slower increase when regular sludge withdrawals were performed. The average  
603 FR in this period was  $5.3 \cdot 10^{11} \text{ m}^{-1} \text{ d}^{-1}$  (Fig. 6b). In Period 2, the  $R_T$  increased to  $6.3 \cdot 10^{12} \text{ m}^{-1}$  after 49  
604 days of operation before the membrane was subjected to a physical-chemical cleaning. The FR  
605 decreased compared to the previous period, resulting equal to  $3.4 \cdot 10^{11} \text{ m}^{-1} \text{ d}^{-1}$  on average. In Period  
606 3, the  $R_T$  reached a maximum value of  $4.1 \cdot 10^{12} \text{ m}^{-1}$  after 48 days of operation, whereas the FR  
607 ( $0.65 \cdot 10^{11} \text{ m}^{-1} \text{ d}^{-1}$ ) was significantly lower compared to what observed in the previous periods. In  
608 Period 4, the  $R_T$  reached its maximum value of  $1.18 \cdot 10^{13} \text{ m}^{-1}$  after 44 days of operation, thereby  
609 showing the highest FR ( $6.15 \cdot 10^{11} \text{ m}^{-1} \text{ d}^{-1}$ ) of the entire experimental campaign. The latter result was  
610 in good agreement with the EPS destruction above discussed, indicating that the destructuration of  
611 the extracellular polymeric matrix was detrimental towards the membrane fouling tendency.

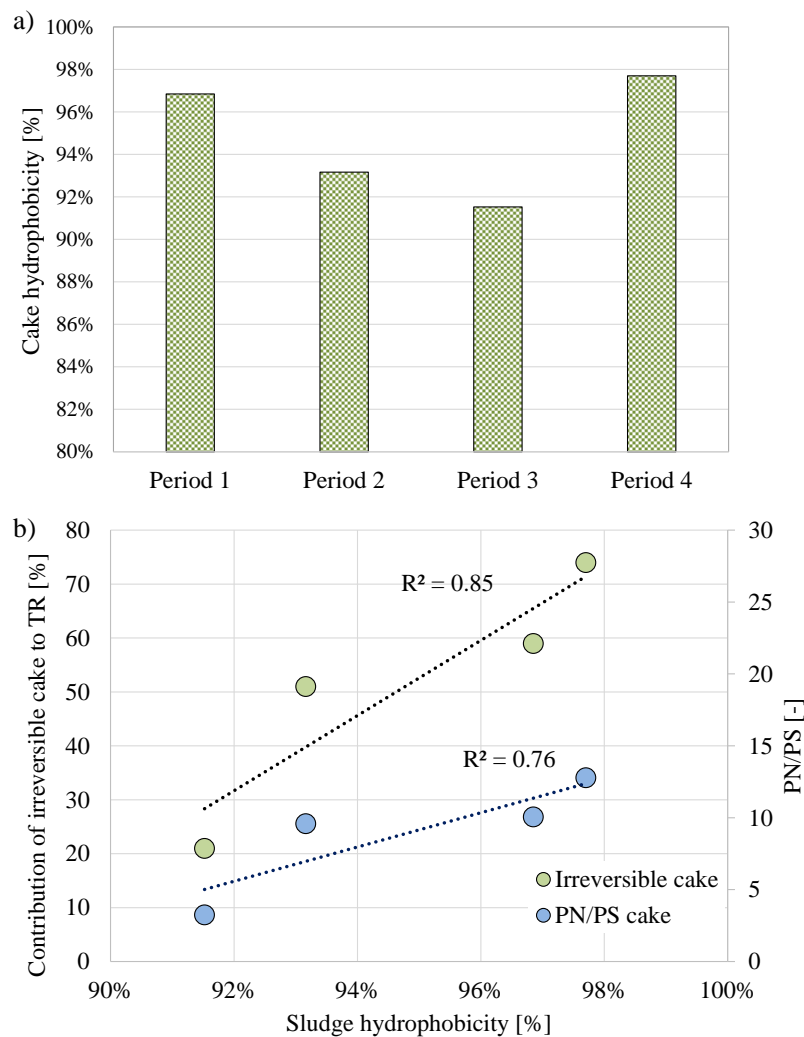
612 The above results confirmed that after the AMSR was implemented, the fouling tendency was  
613 significantly mitigated (de Oliveira et al., 2018). In this light, the optimum HRT of the AMSR was  
614 found to be 8 h, which corresponded to the minimum FR achieved.

615 As noticeable from Figure 6c and Figure 6d, the irreversible cake deposition in Period 1 was the main  
616 fouling mechanism, accounting for approximately 60%, whereas the pore-blocking and the reversible  
617 cake deposition contributed for 24% and 11%. In Period 2, the contribution of the irreversible cake  
618 decreased to 51%, whilst those of pore-blocking and reversible cake increased to 30% and 22%,  
619 respectively. In Period 3, the irreversible cake contribution significantly decreased (21%), while that  
620 of the pore-blocking and the reversible cake increased to 41% and 39%, respectively. Lastly, in Period  
621 4 the fouling mechanism was similar to what observed in Period 1, with the irreversible cake  
622 deposition, the pore-blocking and the reversible cake deposition accounting for 74%, 16%, 13%  
623 respectively.

624 Concerning the membrane service-life preservation, it is of paramount importance to minimize the  
625 pore-blocking mechanism or, alternatively, maximize the recovery of the membrane permeability

626 with chemical cleaning operations. The highest value of the “irremovable fouling”, defined as the  
627 residual portion of fouling after chemical cleanings (Di Bella and Di Trapani, 2019), was observed in  
628 Period 4, whereas the lowest in Period 1. This result indicated that the integration of the AMSR might  
629 cause a potential decrease in the membrane service-life. Nevertheless, the minimum irreversible pore-  
630 blocking resistance was observed in Period 3, suggesting that a HRT of 8 h in the AMSR resulted the  
631 most suitable value to achieve sludge minimization, while preserving the membrane fouling.  
632 It is worth mentioning that the irreversible cake deposition could significantly decrease the membrane  
633 flux, thereby reducing the plant loading potential (Janus and Ulanicki, 2015). With this respect, the  
634 minimum contribution of the irreversible cake deposition to the overall membrane fouling was  
635 observed in Period 3 (21%). The resistance due to the irreversible cake was found to be in good  
636 agreement with the hydrophobicity of the cake layer (Fig. S1).

637



638

639 **Figure S1:** Hydrophobicity of the cake layer during the four experimental periods (a); relationship  
 640 between the sludge hydrophobicity with the contribution of the irreversible cake to the total  
 641 resistance and the PN/PS.

642

643 Indeed, the minimum value of the cake hydrophobicity was observed in Period 3 (91.7%) in  
 644 correspondence with the lowest contribution of the irreversible cake deposition to membrane fouling.  
 645 In contrast, the maximum cake hydrophobicity was observed in Period 4 (97.7%), when the  
 646 contribution of the irreversible cake deposition was the highest (74%). Referring to the cake layer  
 647 composition, it was observed that the amount of proteinaceous EPS was minimum in Period 3,  
 648 resulting in the lowest PN/PS ratio in terms of both bound (3.5) and soluble (4.3) EPS throughout

649 experiments. In contrast, the PN/PS ratio of the bound EPS was higher in Period 1 (10) and Period 2  
650 (12), whereas the PN/PS in the soluble EPS was approximately equal to that observed in Period 2.  
651 These findings demonstrated that the increase of the irreversible cake resistance was strictly related  
652 to the change of cake composition. The higher was the amount of proteins, the higher resulted the  
653 cake hydrophobicity. Indeed, as confirmed by previous studies, proteins are more hydrophobic than  
654 carbohydrates; therefore, their predominance resulted in the increase in sludge hydrophobicity (Niu  
655 et al., 2016). The high protein concentrations dissolved in the bulk liquid determined a significant  
656 presence of proteins on membrane surface, because of the establishment of hydrophobic interactions  
657 with the material of the membrane fibers (PDVF).

658

### 659 *3.6 Mechanism of sludge minimization in the AMSR and implications on the system performances*

660 The findings achieved in the present study demonstrated the effectiveness of integrating the AMSR  
661 for the simultaneous achievement of sludge minimization and phosphorous removal, enabling higher  
662 efficiency compared to ASSR configuration (Kim et al., 2012; Ferrentino et al., 2014; de Oliveira et  
663 al., 2018). Based on the above results, the AMSR integration enabled a significant decrease of sludge  
664 production with the HRT increase in the anaerobic reactor. More precisely, the proper HRT was found  
665 to be 8 h that compensated the excess sludge minimization with the worsening of the effluent quality  
666 and the membrane fouling tendency occurring under higher HRT (10 h). The mechanisms involved  
667 in sludge minimization were different, which operated simultaneously, making it difficult to identify  
668 the prevailing one. Indeed, the bacterial decay increased with the HRT in the AMSR as evidenced by  
669 the significant decrease in the heterotrophic active fraction and the increase in the endogenous decay  
670 rate. Moreover, another mechanism involved in the sludge minimization was the selection of slow  
671 growing bacteria (PAO). Indeed, in Period 2 ad Period 3, a very high activity of PAO was observed,  
672 indicating that the amount of these microorganisms in the activated sludge significantly increased  
673 when the AMSR was integrated in the original MBR layout. Therefore, the TP removal significantly  
674 increased up to 97%, with  $\text{PO}_4\text{-P}$  concentration in the effluent close to  $0.5 \text{ mg L}^{-1}$ . Besides, kinetic



675 tests highlighted that phosphorous release occurred under endogenous conditions, without an external  
676 carbon source. This result was likely due to cell lysis that released biodegradable low molecular  
677 weight compounds utilized by bacteria as a secondary substrate, suggesting the existence of the  
678 cryptic growth process (Quan et al., 2012). Lastly, it should be taken into account that the sludge  
679 cycling between anaerobic and aerobic conditions provided a basis for the energy uncoupling  
680 mechanism and the feasting/fasting conditions that contributed to the excess sludge minimization.

681 Although the sludge minimization efficiency increased with the HRT in the AMSR, it was noted that  
682 prolonged anaerobic-endogenous conditions were detrimental for both the nutrients removal  
683 performances, including the phosphorous, and the membrane fouling tendency. Indeed, the excessive  
684 decrease of the heterotrophic active fraction, the accumulation of endogenous residue, as well as the  
685 destruction of EPS, contributed to worsen the effluent quality. Moreover, under HRT higher than 8  
686 h, the huge increase of proteinaceous EPS and SMP in the membrane cake layer promoted a dramatic  
687 increase in the membrane fouling rate and the irreversible cake deposition, thereby limiting the  
688 applicable flux.

689 Our findings demonstrated that the integration of the AMSR is a valuable management solution to  
690 achieve sludge minimization, although prolonged anaerobic-endogenous conditions are not  
691 encouraged to ensure that neither the effluent quality nor the hydraulic functionality of the membrane  
692 are compromised.

### 693 **Conclusions**

694 The simultaneous achievement of sludge minimization and phosphorous removal was studied in a  
695 novel AMSR-MBR scheme. The AMSR-MBR enabled a sludge reduction of 64% and the highest  
696 removal performance of organic carbon (98%), nitrogen (90%) and phosphorous (97%), as well as  
697 the lowest membrane fouling tendency ( $FR=0.65 \cdot 10^{11} \text{ m}^{-1} \text{ d}^{-1}$ ). Our findings suggested that the  
698 mechanism driving phosphorous removal in the AMSR could involve the cryptic growth process: the  
699 use of the biodegradable low molecular weight compounds deriving from the bacterial lysis, as

700 secondary substrate by PAO, favored the simultaneous achievement of phosphorous removal and  
701 sludge minimization.

702

### 703 **Acknowledgments**

704 Authors warmly thank Eng. Letizia Macellaro La Franca for her precious help and contribution  
705 provided during the pilot plant operations.

706

### 707 **References**

708 APHA, 2005. Standard Methods for the Examination of Water & Wastewater, American Public  
709 Health Association.

710 Campo, R., Capodici, M., Di Bella, G., Torregrossa, M., 2017. The role of EPS in the foaming and  
711 fouling for a MBR operated in intermittent aeration conditions. *Biochem. Eng. J.* 118, 41–52.

712 <https://doi.org/10.1016/j.bej.2016.11.012>

713 Capodici, M., Di Bella, G., Di Trapani, D., Torregrossa, M., 2015. Pilot scale experiment with MBR  
714 operated in intermittent aeration condition: Analysis of biological performance. *Bioresour.*

715 *Technol.* 117, 398-405, <https://doi.org/10.1016/j.biortech.2014.11.075>

716 Capodici, M., Fabio Corsino, S., Di Pippo, F., Di Trapani, D., Torregrossa, M., 2016. An innovative  
717 respirometric method to assess the autotrophic active fraction: Application to an alternate

718 oxic–anoxic MBR pilot plant. *Chem. Eng. J.* 300, 367–375.

719 <https://doi.org/10.1016/j.cej.2016.04.134>

720 Cheng, C., Zhou, Z., Niu, T., An, Y., Shen, X., Pan, W., Chen, Z., Liu, J., 2017. Effects of side-  
721 stream ratio on sludge reduction and microbial structures of anaerobic side-stream reactor

722 coupled membrane bioreactors. *Bioresour. Technol.* 324, 380–388.

723 <https://doi.org/10.1016/j.biortech.2018.07.097>

724 Chuang, S.H., Chang, W.C., Huang, Y.H., Tseng, C.C., Tai, C.C., 2011. Effects of different carbon

725 supplements on phosphorus removal in low C/P ratio industrial wastewater. *Bioresour.*  
726 *Technol.* 102, 5461–5465. <https://doi.org/10.1016/j.biortech.2010.11.118>

727 Chudoba, P., Morel, A., Capdeville, B., 1992. The case of both energetic uncoupling and metabolic  
728 selection of microorganisms in the oxa activated sludge system. *Environ. Technol.* (United  
729 Kingdom) 13, 761–770. <https://doi.org/10.1080/09593339209385207>

730 Coma, M., Rovira, S., Canals, J., Colprim, J., 2015. Integrated side-stream reactor for biological  
731 nutrient removal and minimization of sludge production. *Water Sci. Technol.* 71, 1056–1064.  
732 <https://doi.org/10.2166/wst.2015.067>

733 Datta, T., Liu, Y., Goel, R., 2009. Evaluation of simultaneous nutrient removal and sludge reduction  
734 using laboratory scale sequencing batch reactors. *Chemosphere* 76, 697–705.  
735 <https://doi.org/10.1016/j.chemosphere.2009.02.040>

736 de Oliveira, T.S., Corsino, S.F., Di Trapani, D., Torregrossa, M., Viviani, G., 2018. Biological  
737 minimization of excess sludge in a membrane bioreactor: Effect of plant configuration on  
738 sludge production, nutrient removal efficiency and membrane fouling tendency. *Bioresour.*  
739 *Technol.* 259, 146-155. doi:10.1016/j.biortech.2018.03.035

740 Devlin, T.R., di Biase, A., Kowalski, M., Oleszkiewicz, J.A., 2016. Granulation of activated sludge  
741 under low hydrodynamic shear and different wastewater characteristics. *Bioresour. Technol.*  
742 224, 1–7. <https://doi.org/10.1016/j.biortech.2016.11.005>

743 Di Bella, G., Di Trapani, D., 2019. A brief review on the resistance-in-series model in membrane  
744 bioreactors (MBRs). *Membranes* 9(2), 24. <https://doi.org/10.3390/membranes9020024>.

745 DuBois, M., Gilles, K. a., Hamilton, J.K., Rebers, P. a., Smith, F., 1956. Colorimetric method for  
746 determination of sugars and related substances. *Anal. Chem.* 28, 350–356.  
747 <https://doi.org/10.1021/ac60111a017>

748 Ferrentino, R., Langone, M., Andreottola, G., Rada, E.C., 2014. An anaerobic side-stream reactor in  
749 wastewater treatment: A review. *WIT Trans. Ecol. Environ.* 191, 1435–1446.

750 <https://doi.org/10.2495/SC141212>

751 Ferrentino, R., Langone, M., Merzari, F., Tramonte, L., Andreottola, G., 2016. A review of  
752 anaerobic side-stream reactor for excess sludge reduction: Configurations, mechanisms, and  
753 efficiency. *Crit. Rev. Environ. Sci. Technol.* 46 (4), 382-415.  
754 [doi:10.1080/10643389.2015.1096879](https://doi.org/10.1080/10643389.2015.1096879)

755 Foladori, P., Andreottola, G., Ziglio, G., 2010. *Sludge Reduction Technologies in Wastewater*  
756 *Treatment Plants*. IWA Publishing. ISBN: 9781780401706.  
757 <https://doi.org/10.2166/9781780401706>

758 Goel, R.K., Noguera, D.R., 2006. Evaluation of Sludge Yield and Phosphorus Removal in a  
759 Cannibal Solids Reduction Process. *J. Environ. Eng.* 132, 1331–1338.  
760 [https://doi.org/10.1061/\(asce\)0733-9372\(2006\)132:10\(1331\)](https://doi.org/10.1061/(asce)0733-9372(2006)132:10(1331))

761 Ioannou-Ttofa, L., Foteinis, S., Chatzisyneon, E., Fatta-Kassinou, D., 2016. The environmental  
762 footprint of a membrane bioreactor treatment process through Life Cycle Analysis. *Sci. Total*  
763 *Environ.* 568, 306–318. <https://doi.org/10.1016/j.scitotenv.2016.06.032>

764 Janus, T., Ulanicki, B., 2015. A behavioural membrane fouling model for integrated simulation of  
765 membrane bioreactors for wastewater treatment, in: *Procedia Engineering*. pp. 1328–1337.  
766 <https://doi.org/10.1016/j.proeng.2015.08.964>

767 Kim, Y.M., Chon, D.H., Kim, H.S., Park, C., 2012. Investigation of bacterial community in  
768 activated sludge with an anaerobic side-stream reactor (ASSR) to decrease the generation of  
769 excess sludge. *Water Res.* 46, 4292–4300. <https://doi.org/10.1016/j.watres.2012.04.040>

770 Le-Clech, P., Chen, V., Fane, T.A.G., 2006. Fouling in membrane bioreactors used in wastewater  
771 treatment. *J. Memb. Sci.* 284 (1-2), 17-53. [doi:10.1016/j.memsci.2006.08.019](https://doi.org/10.1016/j.memsci.2006.08.019)

772 Lowry, O.H., Rosebrough, N.J., Farr, A.L., Randall, R.J., 1951. Protein measurement with the  
773 Folin-Phenol Reagent. *J. Biol. Chemistry* 193, 265–275.

774 Moreira, I.S., Amorim, C.L., Ribeiro, A.R., Mesquita, R.B.R., Rangel, A.O.S.S., Loosdrecht,

775 M.C.M. Van, Tiritan, M.E., Castro, P.M.L., 2015. Removal of fluoxetine and its effects in the  
776 performance of an aerobic granular sludge sequential batch reactor. *J. Hazard. Mater.* 287, 93–  
777 101. <https://doi.org/10.1016/j.jhazmat.2015.01.020>

778 Niu, Z., Zhang, Z., Liu, S., Miyoshi, T., Matsuyama, H., Ni, J., 2016. Discrepant membrane fouling  
779 of partial nitrification and anammox membrane bioreactor operated at the same nitrogen  
780 loading rate. *Bioresour. Technol.* 214, 729–736. <https://doi.org/10.1016/j.biortech.2016.05.022>

781 Pronk, M., de Kreuk, M.K., de Bruin, B., Kamminga, P., Kleerebezem, R., van Loosdrecht,  
782 M.C.M., 2015. Full scale performance of the aerobic granular sludge process for sewage  
783 treatment. *Water Res.* 84, 207–217. <https://doi.org/10.1016/j.watres.2015.07.011>

784 Quan, F., Anfeng, Y., Libing, C., Hongzhang, C., Xing, X.H., 2012. Mechanistic study of on-site  
785 sludge reduction in a baffled bioreactor consisting of three series of alternating aerobic and  
786 anaerobic compartments. *Biochem. Eng. J.* 67, 45–51.  
787 <https://doi.org/10.1016/j.bej.2012.05.006>

788 Ramdani, A., Dold, P., Gadbois, A., Déléris, S., Houweling, D., Comeau, Y., 2012. Biodegradation  
789 of the endogenous residue of activated sludge in a membrane bioreactor with continuous or on-  
790 off aeration. *Water Res.* 46, 2837–2850. <https://doi.org/10.1016/j.watres.2012.01.008>

791 Rosenberg, M., 1984. Bacterial adherence to hydrocarbons: a useful technique for studying cell  
792 surface hydrophobicity. *FEMS Microbiol. Lett.* 22, 289–295. [https://doi.org/10.1111/j.1574-  
793 6968.1984.tb00743.x](https://doi.org/10.1111/j.1574-6968.1984.tb00743.x)

794 Saby, S., Djafer, M., Chen, G.H., 2003. Effect of low ORP in anoxic sludge zone on excess sludge  
795 production in oxic-settling-anoxic activated sludge process. *Water Res.* 37, 11–20.  
796 [https://doi.org/10.1016/S0043-1354\(02\)00253-1](https://doi.org/10.1016/S0043-1354(02)00253-1)

797 Safwat, S.M., 2018. Performance of moving bed biofilm reactor using effective microorganisms. *J.*  
798 *Clean. Prod.* 185, 723–731. <https://doi.org/10.1016/j.jclepro.2018.03.041>

799 Sarioglu, M., Sayi-Ucar, N., Cokgor, E., Orhon, D., van Loosdrecht, M.C.M., Insel, G., 2017.

800 Dynamic modeling of nutrient removal by a MBR operated at elevated temperatures. *Water*  
801 *Res.* 123, 420–428. <https://doi.org/10.1016/j.watres.2017.07.001>

802 Semblante, G.U., Hai, F.I., Bustamante, H., Guevara, N., Price, W.E., Nghiem, L.D., 2016a.  
803 Biosolids reduction by the oxic-settling-anoxic process: Impact of sludge interchange rate.  
804 *Bioresour. Technol.* 210, 167–173. <https://doi.org/10.1016/j.biortech.2016.01.010>

805 Semblante, G.U., Hai, F.I., Bustamante, H., Price, W.E., Nghiem, L.D., 2016b. Effects of sludge  
806 retention time on oxic-settling-anoxic process performance: Biosolids reduction and  
807 dewatering properties. *Bioresour. Technol.* 218, 1187–1194.  
808 <https://doi.org/10.1016/j.biortech.2016.07.061>

809 Semblante, G.U., Hai, F.I., Bustamante, H., Price, W.E., Nghiem, L.D., 2016c. Effects of sludge  
810 retention time on oxic-settling-anoxic process performance: Biosolids reduction and  
811 dewatering properties. *Bioresour. Technol.* 218, 1187–1194.  
812 <https://doi.org/10.1016/j.biortech.2016.07.061>

813 Semblante, G.U., Hai, F.I., Ngo, H.H., Guo, W., You, S.J., Price, W.E., Nghiem, L.D., 2014.  
814 Sludge cycling between aerobic, anoxic and anaerobic regimes to reduce sludge production  
815 during wastewater treatment: Performance, mechanisms, and implications. *Bioresour. Technol.*  
816 [doi:10.1016/j.biortech.2014.01.029](https://doi.org/10.1016/j.biortech.2014.01.029)

817 Troiani, C., Eusebi, A.L., Battistoni, P., 2011. Excess sludge reduction by biological way: From  
818 experimental experience to a real full scale application. *Bioresour. Technol.* 102, 10352–  
819 10358. <https://doi.org/10.1016/j.biortech.2011.08.124>

820 Velho, V.F., Foladori, P., Andreottola, G., Costa, R.H.R., 2016. Anaerobic side-stream reactor for  
821 excess sludge reduction: 5-year management of a full-scale plant. *J. Environ. Manage.* 177,  
822 223–230. <https://doi.org/10.1016/j.jenvman.2016.04.020>

823 Wang, Z., Yu, H., Ma, J., Zheng, X., Wu, Z., 2013. Recent advances in membrane bio-technologies  
824 for sludge reduction and treatment. *Biotechnol. Adv.* 31, 1187-1199.

825 doi:10.1016/j.biotechadv.2013.02.004

826 Ye, F.X., Zhu, R.F., Li, Y., 2008. Effect of sludge retention time in sludge holding tank on excess  
827 sludge production in the oxic-settling-anoxic (OSA) activated sludge process. *J. Chem.*  
828 *Technol. Biotechnol.* 83, 109–114. <https://doi.org/10.1002/jctb.1781>

829 Zuthi, M.F.R., Guo, W.S., Ngo, H.H., Nghiem, L.D., Hai, F.I., 2013. Enhanced biological  
830 phosphorus removal and its modeling for the activated sludge and membrane bioreactor  
831 processes. *Bioresour. Technol.* 139, 363-374. doi:10.1016/j.biortech.2013.04.038

832

833

834 **Figure caption**

835 **Figure 1:** Trends of TSS concentration and VSS/TSS ratio during the experiment

836 **Figure 2:** Average values of the observed yield coefficient ( $Y_{obs}$ ), the maximum yield coefficient  
837 ( $Y_H$ ) and their respective percentage reduction obtained in the four experimental periods.

838 **Fig. 3:** Trends of the COD concentration in the influent, in the supernatant of the anoxic, aerobic and  
839 AMSR and in the permeate (a); biological and overall COD removal efficiency and effluent COD  
840 concentration (b); ammonia nitrogen in the influent and in the supernatant of each reactor (c); TN  
841 removal efficiency and TN concentration (as nitrate) in the permeate (d);  $PO_4$ -P concentration in the  
842 influent, in the supernatant of each reactor (e); TP removal efficiency and  $PO_4$ -P concentration in the  
843 permeate.

844 **Figure 4:** Results of the kinetic tests carried out in Period 1 (a), Period 2 (b), Period 3 (c) and Period  
845 (4).

846 **Figure 5:** Average EPS content in the anoxic, aerobic and AMSR during the four experimental  
847 periods

848 **Figure 6:** The trend of the total resistance of the membrane (a), the average fouling rate during the  
849 four experimental periods (b), the total resistance decomposition (c), and the contribution of each  
850 fouling mechanism to the overall membrane fouling (d).

851 **Figure S1:** Hydrophobicity of the cake layer during the four experimental periods (a); relationship  
852 between the sludge hydrophobicity with the contribution of the irreversible cake to the total resistance  
853 and the PN/PS.

854

855 **Table caption**

856 **Table 1:** Summary of the wastewater characteristics and the main operating conditions of the MBR

857 **Table 2:** Summary of the main biokinetics parameters of the OHO.